CLM-P604

CLM-P604

UKAEA

Preprint

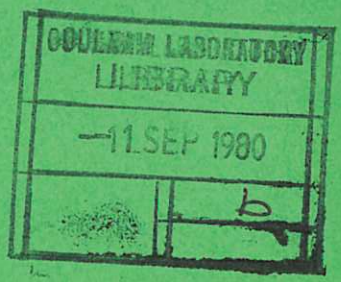

RELIABLE PRODUCTION OF ISOLATED DEUTERIUM PELLETS FOR LASER-GENERATED PLASMA EXPERIMENTS

S. KOGOSHI
I. J. SPALDING
A. C. WALKER
S. WARD

CULHAM LABORATORY
Abingdon Oxfordshire

1980

CLM-P 604

RELIABLE PRODUCTION OF ISOLATED DEUTERIUM PELLETS FOR LASER-GENERATED PLASMA EXPERIMENTS

S. Kogoshi*, I.J. Spalding, A.C. Walker and S. Ward

Culham Laboratory
Abingdon, Oxon, OX14 3DB, UK
(Euratom/UKAEA Fusion Association)

ABSTRACT

The performance of an improved cryogenic device, designed to drop isolated pellets of solid deuterium to the fixed focus of a high energy laser for low-Z plasma generation, is described. > 99% interception of pellets has been achieved for a fall of 30 cm in the absence of external mechanical disturbance. The factors affecting this spatial accuracy and also the exact timing of the pellet fall are discussed, as well as the reproducibility of the pellet mass.

Short title: Production of Deuterium Pellets

INSPEC: 07.20M

*Present address: Department Electrical Engineering, Tokyo University, Japan.

(Submitted for publication in J. Phys. E: Sci. Instrum.)

MARCH 1980

1. Introduction

Laser-plasma filling experiments on both Culham's CLEO and the IPP, Garching WIIb Stellarators provided the motivation for development of a cryogenic device at IPP capable of producing isolated deuterium pellets suitable for laser irradiation (Baumhacker et al. 1976, Amenda 1977). The Garching/Culham collaboration resulted in the design of a miniaturised version of this prototype manufactured by Leybold-Heraeus. The miniaturisation was determined primarily by geometrical constraints on CLEO, this being the machine with the most restricted access. Identical machines were supplied to both IPP and Culham.

The purpose of this paper is to summarise experience gained on the operation and performance of this D_2 pellet dropper, in particular detailing modifications and operating techniques which have been found to give significantly improved stability and reproducibility during the course of the CLEO stellarator laser-filling programme.

2. Pellet Dropper

The device is shown in Fig. 1. It is based on a standard continuous-flow liquid helium cryostat. Deuterium gas is condensed in a cylinder and a piston is used to extrude a 300μm diameter cylindrical stick through a nozzle at the bottom. Two heated cutting wires, normal to the axis of the cylinder, then expand and cut off a length of D_2 which drops freely under gravity to the laser focus.

The length of the pellet is controlled by a photo-diode in a screen, onto which an image of the extruding pellet is projected. Shadowing of the diode by the tip of the pellet image immediately stops the extrusion. Adjustment of the diode position sets the required pellet length. A

second diode senses the pellet image passing as it falls and restarts the automatic pellet extrusion/cutting cycle. Adjustable timers set the period between each phase of the cycle.

A standard Leybold-Heraeus temperature controller (ER-3) is used to accurately stabilize the cryostat temperature. Three temperatures are set for various parts of the pellet production cycle: a base temperature; a higher temperature which softens the deuterium for extrusion and an intermediate one used during pellet cutting. A pre-set resistance value is switched into the temperature monitoring resistance bridge (which includes the resistance thermometer) to select each temperature. Extrusion is controlled by temperature changes only, the piston pressure being maintained at a constant value throughout.

2.1 Pellet Dropper Operation

(i) A base pressure of a few 10^{-5} torr is attained before cooling the cryostat. Liquid He is sucked through the cryostat by a pump, the He-dewar pressure remaining at atmospheric. The base temperature of around 6 K is reached in about 10 minutes.

(ii) With the piston raised, deuterium gas is passed into the condensation cylinder and through the nozzle until the latter is sealed by the accumulating frozen gas. The subsequent pressure rise is halted automatically when the filling line reaches ~ 0.5 atmospheres. Condensation of the gas is observed by the return to vacuum in the filling line. The required D_2 fill is achieved by further inlets of gas.

(iii) To commence extrusion the piston is lowered with a pressure of 35 psig in the actuating air cylinder. The cryostat temperature is then raised slowly over a period of about 5 minutes to the extrusion temperature of around 14.5 K (320Ω on the reference resistance).

This allows gradual compression of the D_2 into a uniform density fill. Once a length of deuterium has been extruded, clearing any impurities initially condensed near the nozzle, the base temperature is set at 6 K (65Ω).

The automatic extrusion/cutting cycle is then started using a cutting temperature of typically 12 K (39Ω). The cutting-wire power supplies have adjustable current and voltage limits which permit fine tuning of the pellet cutting. This adjustment, together with the choice of cryostat temperature when cutting, is critical in achieving accurately falling pellets. The aim is to cut symmetrically down to a fine neck, directly above the pellet centre of gravity, which then breaks under the pellet's own weight as the D_2 softens on reaching the cutting temperature. In practice this is done by starting the cut at the base temperature, and with current still passing through the cutting wires, finally raising the temperature. The delay between this final operation and the pellet detaching can be anywhere between 1 second and 20 seconds. In practice there is a trade off between a low time jitter obtained with a short delay after the final 'command' (the temperature rise), and achieving the minimum of spatial scatter of falling pellets, usually achieved with slower cutting. Typically a delay in pellet detachment of about 6 seconds is used.

To achieve stable, reproducible operation the source is operated continuously producing a pellet at intervals of $\frac{1}{2}$ to 2 minutes. It is commonly run for periods of up to 12 hours. The other typical working parameters are given in Table 1.

3. Culham Modifications to Pellet Dropper

The CLEO laser-plasma experiment required a pellet to be dropped ~ 30 cm into a $\frac{1}{2}$ mm diameter He-Ne laser beam, marking the centre of the somewhat larger CO_2 laser focus. High spatial accuracy was therefore required in

one dimension only, as the long focal depth of the CO_2 laser ($\sim$ 1cm) made scatter of a few millimetres along its axis unimportant. Observations on the IPP prototype as well as tests with the Culham device showed that greater scatter of pellets occurs in the direction parallel to the two cutting wires. For this reason the dropper was aligned with this axis close to that of the laser (about 30 degrees in the CLEO experiment).

The second requirement in the CLEO experiment was for a pellet to be dropped within a time interval of 0.5 seconds, corresponding to the period during which the stellarator ℓ winding could be safely energised (the actual 0.25 sec current pulse being triggered by the pellet detaching). This degree of timing accuracy was not intended by the original IPP designers of the machine as the WIIb experiment used dc or long pulse fields and hence the pellet fall time was not critical. Some of the modifications, described in the following, were particularly important in approaching this timing specification. In general the changes were all made to improve the temperature reproducibility of the cryostat for each pellet production cycle. This factor, together with ensuring that the same heater current is flowing in the cutting wires for each pellet cut, is dominant in determining both the spatial and temporal accuracy achieved.

3.1 Liquid Helium Flow Control

The temperature controller can operate with a feedback loop adjusting both the helium flow rate, via an electro-magnetic valve in the helium pump line, and the heat input from an electrical heater. In practice automatic adjustment of the helium flow rate leads to only partly damped instabilities and so it was dispensed with and heater control of the temperature was used on its own. It was further found that any fluctuations in He flow resulted in significant changes in pellet production, despite apparently accurate control of temperature by the heater feedback system. This is believed to be the result of changing temperature gradients within

the cryostat allowing the nozzle temperature to vary slightly from that at the temperature sensing position. To minimise this effect one ideally includes a constant flow feedback on the liquid helium pump system. In the absence of such a control, a best attempt was made at setting reproducible He flow conditions. This was achieved by maintaining both the He dewar and the pump line at constant pressure - 1 atmosphere and 600 torr respectively. In addition the electro-magnetic valve in the pump line was removed, the flow being throttled by a simpler and more reliable mechanical valve.

3.2 Heater Control

A shortcoming in the temperature controller arises from it being designed to stabilize one particular temperature only. In particular, the heater control (a simple 1kΩ potentiometer), which sets an average heat input to be modulated as required for constant temperature, can be optimised for only one of the three temperatures selected. Thus when a different resistance value is switched into the reference bridge the controller fails to stabilize the temperature accurately on the value required.

To solve this problem, two extra potentiometers plus the necessary relays were added to the controller so that as each of the three temperatures are selected the corresponding (optimised) heater-current is switched in.

3.3 Maximum Temperature Limit

It was found that occasional false triggering of the control photo-diodes (due to changes in ambient light or electrical noise) or a change in the helium flow rate could sometimes result in incorrect sequencing of the various pellet production phases and cause two or three different temperatures to be selected simultaneously. This has the effect of connecting in parallel the pre-set reference resistors into the temperature controller

bridge. The low effective resistance thus obtained is equivalent to setting a high temperature and as a result the condensed deuterium is rapidly vaporised. Thus a brief interruption in operation becomes a more serious halt, necessitating re-filling with deuterium before continuing. This has now been prevented simply by the addition of a common series resistance close to the lowest value required ($\sim 31\Omega$) which limits the maximum temperature that can be achieved.

3.4 Cutting Wire Monitoring

The power dissipated in each cutting wire is critical both to pellet scatter and the delay in pellet detachment. The two power supplies feeding these wires have analogue meters for monitoring both voltage and current, accurate to $\sim$ 10%. It has been found useful to supplement these with digital meters accurate to four significant figures. This allows precise monitoring of the resistance of the wires (which is a function of their temperature) and permits more accurate compensation for any changes in this value. Section 4.3(c) discusses in greater detail the temperature changes experienced by the cutting wires.

3.5 External Timing Control

The internal timing of the pellet production cycle is based on adjustable delays separating the completion of one phase and the start of the next. As the duration of each phase (e.g. the time between starting extrusion and reaching the required pellet length) is variable, the total cycle time is unpredictable. In order to synchronize a separate event with the pellet fall, in particular the firing of CLEO stellarator, an external timer was used both to control the pellet cycle and initiate the firing sequences of the stellarator and the laser. The start of each phase of the cycle was then pre-set, after allowing sufficient time for completion of the previous process.

This technique, by giving independent control over the timing of each phase, was also found to be advantageous when setting up for minimum pellet scatter and time jitter.

4. Performance of Modified Pellet Dropper

Combination of all the modifications detailed in the previous section has resulted in significantly improved performance over that of the original prototype. In particular pellet/laser interception probability has been raised to almost 100%, in the absence of any externally originating mechanical disturbances.

4.1 Spatial Scatter of Pellets

As already indicated the critical scatter direction is that perpendicular to the laser axis. In this direction the pellet must pass within a 0.5 mm wide spot after a fall of 30 cm. With the Garching prototype and the unmodified Culham device this was achieved with a probability of around 50%. Using the modified source, in a run of 105 consecutive pellets, dropped over a period of two hours, 104 were detected. This result is typical of operation on CLEO when the stellarator was not being fired. However, energizing the CLEO toroidal field coils results in movements of both the pellet dropper and the detection optics, due to incomplete mechanical de-coupling, and the final probability of a pellet falling with the required accuracy was reduced to around 75% (averaged over 87 pellets dropped).

Despite their reproducibile trajectory it has been found that the pellets tumble in a random fashion as they fall, due to imperfect detachment. This is illustrated in Fig. 2b, which shows a shadow graph of a pellet taken as it passes through the detection point.

4.2 Jitter in Pellet Detachment Time

The delay between initiating the final temperature rise and detachment of

the pellet (tc) is determined by a number of factors:-

a) the cryostat cutting temperature,

b) the temperature of the cutting wires - determined by the voltage/current settings and the ratio of their 'on' to 'off' times,

c) the weight of the deuterium pellet - determined by the extrusion temperature (which affects its diameter) as well as the pellet length.

Fig. 3 illustrates the dependence of the cutting time (tc) on cutting temperature (Tc). Fig. 4a shows the dependence of pellet diameter on extrusion temperature which is the cause of the variation of cutting time with this parameter shown in Fig. 4b. Similarly an increase in pellet length also increases the pellet mass, and hence reduces the cutting time as shown in Fig. 5. The cutting wire performance is described in more detail in the next section.

A small change in any of these factors can alter the precise time at which the pellet drops. As a result careful control of the complete cycle is essential for reproducible pellet timing to be achieved.

When operating with minimal spatial scatter ($\gtrsim$ 99% pellet detection rate), the jitter in pellet fall time is typically $\pm$ 7%. In the CLEO experiment, where again machine movements affected the fall, 50% of the pellets were dropped into the necessary 0.5 s interval.

4.3 Long Term Drift

It was found that despite apparently good temperature reproducibility the cutting time (tc)(and possibly the spatial scatter, to a smaller extent) drifted steadily from its initial value at up to 1 s/hr. Unlike the changes in tc caused by random fluctuations of the various critical parameters, this systematic error can be compensated for. However, more frequent attention from the operator is then required and therefore an attempt has been made

to understand this drift in the hope of eliminating it.

Three factors can be identified as possible contributors to the long term drift.

a) Liquid Helium Flow Changes

As already indicated a change in the helium flow rate may result in a different deuterium temperature due to temperature gradients between the sensing thermometer and the extrusion nozzle. If this change is a steady shift in one direction it can contribute to the observed drift in cutting time. In practice such a flow change is indeed indicated by an observed fall of pressure on the pump side of the cryostat flow-line at a rate of ~ 3.3 torr per hour. Since the pressure in the helium dewar is kept constant this must be due to steady changes in pump efficiency, flow resistance or liquid helium level. The latter typically falls at a rate of 4 cm/hr, corresponding to a pressure drop of 0.6 torr/hr, and thus it cannot alone account for the observed change. A servo-controlled liquid helium flow controller would probably compensate for this drift factor.

b) Cutting Wire Voltage Changes

For a particular power supply setting (of around 1 volt) a drift of $\lesssim$ 12mV/hr is observed on the digital meters, corresponding to a cutting time change of up to 0.4 s/hr. This could be eliminated by greater stabilization of the supply.

c) Cutting Wire Temperature Changes

In addition to changes in the applied voltage the cutting wire temperature can be varied by altering the relative times during which the current is on and off. Fig. 6 shows this change of cutting wire resistance (determined by the temperature) over a period of nearly two hours. At first the ratio of wire heating time to cooling time is around 1 and a steady increase in temperature is seen for the first ~ 1 hour. After this period the duty ratio is dropped to 0.8, and the temperature is seen to drop and approach a steady state value. This effect is analysed in more detail in the calculations described in the appendix.

Fig. 7 shows the good agreement obtained between the calculated and experimentally observed current waveforms for a single cutting cycle. Fig. 8 demonstrates qualitatively how the mean cutting wire temperature can steadily drift up over a number of cycles with the 'on' to 'off' ratio equalling unity, as in the first half of Fig. 6. The calculated time constant for equilibrium to be reached is somewhat shorter than that observed in practice: however, the model clearly demonstrates the importance of optimizing this ratio to reduce long term drifts. (Typically a ratio of $\sim$ 0.8 has been used, as in the second half of Fig. 6).

4.4 Deuterium Ice Density and Total Particle Number

The total particle number was deduced by observing the pressure rise with a 'Baratron' gauge after a pellet is dropped into a chamber of known volume. Suitable corrections were made to allow for outgassing and small leaks into the chamber, giving a systematic error of $\pm$ 8%.

To determine the particle density, a measure of the pellet volume is required. Fig. 2a shows the image of the pellet viewed by the TV camera (recorded on video-tape) from which an estimate of the volume is made. Given the complex shape plus the accumulation of linear measurement errors, the accuracy for a single pellet, can be no better than 13%. However, the measured pressure rise for consecutive pellets was found to vary by less than 1% Thus the statistical errors were reduced by averaging over a number of pellets and a final accuracy of $\pm$ 16% was deduced: giving a particle density of $(5.8 \pm 0.9) \times 10^{22}$ atoms cm^{-3}. This agrees well with the published value of 6.0×10^{22} atoms cm^{-3} at a temperature of 12 K (Roder et al. 1973) confirming that the pellet is indeed solid deuterium and not a lower density 'snow'.

Thus, using the published density value, the particle number in any particular pellet can be calculated from its known volume, typically to

an accuracy of about ± 15%. The two main techniques for changing the volume are: alteration of the extrusion length or extrusion temperature. The effect of the latter (which changes the pellet diameter) is demonstrated in Table 2.

5. Conclusion

Under optimum conditions it has been demonstrated that by careful regulation of the cryostat and cutting wire temperatures solid deuterium pellets (300μm diameter by 600-900μm long) can be dropped 30 cm from the Leybold-Heraeus source to a 0.5 mm diameter laser focal region with a reliability of $\gtrsim$ 99%. Over 50% of the pellets can be dropped into a pre-determined half-second interval. The measured density of these pellets agrees well with published values and it has been shown that the mass of consecutive pellets can vary by as little as 1%.

In conjunction with the TROJAN CO_2 laser, the device has successfully permitted the generation of current-less, highly-ionised, plasmas within CLEO with initial electron densities of up to 2×10^{19} m^{-3} and ion kinetic energies of $\sim$ 600 eV (Walker et al. 1978, Atkinson et al. 1979). With the cryostat vacuum pump between the pellet source and the stellarator no significant change in the torus pressure, $\sim 5 \times 10^{-8}$ torr, was observed during pellet extrusion and cutting.

The pellet dropper has also acted as a source for preliminary studies of the laser-acceleration of D_2 pellets to the velocities required for fusion-reactor refuelling (Burgess et al. 1978). The pellet source at IPP has also been used successfully to generate a plasma within the WIIb stellarator (Baumhacker et al. 1977) and for fuelling experiments on Pulsator (Amenda et al. 1977).

It is believed that the modifications to the pellet dropper, detailed above, permit it to perform more reliably than both the original IPP prototype and a D_2-pellet source recently constructed in Japan (Sato et al. 1977).

Acknowledgements

The authors wish to record their gratitude to Dr. M. Salvat and the late Dr. W. Riedmuller for their cooperation and assistance in the design of this device, based on their prototype. In addition, we thank Mr. R. Hunt for his assistance in the final design stage: Dr. T. Stamatakis for useful discussions and Messrs. B. Willis and A. McKenzie-Wintle for their technical support.

Table 1

Typical working conditions of the pellet dropper

(1) Extruding temp. (T_E)	14.5 K
(2) Base temp. (T_B)	6.0 K
(3) Cutting temp. (T_C)	12.0 K
(4) Supply voltage to cutting wires	
Left	1.2 V
Right	1.3 V
(5) Heating time of cutting wire	(t_h) 32 s
(6) Cooling time of cutting wire	(t_{co}) 41 s
(7) Pressure on extruding piston (P)	35 psi
(8) Liquid helium flow rate	6-7 l/h

Table 2

Dependence of the total number of atoms in a deuterium Pellet on the Extruding temp. (T_E). (T_B 6.7 K, T_C 10.7 K)

T_E (K)	14.0	13.3	12.7
$\overline{N}$ (atoms)	4.8×10^{18}	4.1×10^{18}	3.7×10^{18}

References

Amenda W 1977 Construction of the pellet source for the WIIb stellarator and first phase of operation.
Garching Report IPP 4/151.

Amenda W et al. 1977 Pellet ablation studies at Garching.
Proc. Fusion Fueling Workshop (Princeton) 110.

Atkinson D W et al. 1979 Confinement of low and zero current plasma in the CLEO stellarator.
Proc. 9th European Conference on Controlled Fusion and Plasma Physics, Oxford 6.

Baumhacker et al. 1976 Experiments for filling magnetic confinement machines with laser produced plasma. Preliminary Results.
Proc. 9th Symp. Fusion Tech. 873.

Baumhacker et al. 1977 First results on the confinement of a laser-produced plasma in the WIIb stellarator.
Proc. 8th European Conference on Controlled Fusion and Plasma Physics, Prague, Vol. 1 133.

Burgess M D J et al. 1979 Acceleration of macroparticles by laser light, Plas. Phys. and Cont. Nucl. Fusion Research, Nucl. Fusion Suppl., Vol III 921.

Roder H M et al. 1973 Survey of the properties of the hydrogen isotopes below their critical temperatures,
NBS Technical Note 641.

Sato K N et al. 1977 High-temperature high-quality deuterium plamsa production by laser beams and interactions with magnetic fields.
Plas. Phys. and Cont. Nucl. Fusion Research, Nucl. Fusion Suppl. Vol II 567.

Smithells C J 1962 Metals reference book 3rd Edition
(Butterworth & Co.) Vol. 2 719.

Walker A C et al. 1978 Production of isolated, energetic, D_2 plasmas by CO_2 lasers.
Optics Commun. 27 247.

Appendix

The power supply may be assumed to operate in a constant voltage mode, feeding the tungsten cutting wires through copper connecting wires via the stainless steel support terminals. The temperature achieved is then determined mainly by the current flowing, radiation losses and conduction losses to the supports and supply wires. Thus the equations governing the cutting wire temperature (Tw) may be written as follows:

$$C_w \frac{dT_W}{dt} \simeq I^2 R_w - \alpha_w \sigma S_w T_w^4 - 2b_{eff} (T_w - T_s) \quad (1)$$

$$C_s \frac{dT_s}{dt} \simeq I^2 R_s - \alpha_s \sigma S_s T_s^4 + b_{eff} (T_w - T_s) - \frac{Ka}{L} (T_s - T_o) \quad (2)$$

$$I \simeq \frac{V_o}{R_w + R_s + R_o} \quad (3)$$

$C_w \simeq 0.8 \times 10^{-3}$ J K^{-1}, and $C_s \simeq 0.11$ J K^{-1}, are the heat capacities of the cutting wire and support respectively.

T_w, and T_s, are the respective temperatures of the cutting wire and its support.

I, is the current.

R_w, is the cutting wire resistance equalling $\sim (0.03\ T_w - 4.28)\ L/S \times 10^{-6}$ ohms. (where L is its length and S is the cross section area).

R_s, is the resistance of the support terminal and is approximately 0.02 ohms.

α_w and α_s, are the emissivities of tungsten and stainless steel respectively both being ~ 0.1, (Smithells 1962).

σ, is the black-body radiation coefficient $\sim 5.7 \times 10^{-8}$ W m^{-2} K^{-4}.

S_w and S_s, are the surface areas of the cutting wire and supports, respectively $S_w \sim 0.97 \times 10^{-5}$ m^2 and $S_s \sim 2.8 \times 10^{-4}$ cm^2.

b_{eff} is an effective thermal conduction between the wires and the support.

$\frac{Ka}{L}$ is the thermal conduction along the connecting copper wires, $\sim 1.2 \times 10^{-4}$ JK^{-1}

T_o is room temperature $\sim$ 300K.

V_o and R_o, are the power supply voltage and internal resistance (including the connecting wires).

The one unknown, b_{eff}, is deduced experimentally in the following way. In equilibrium, equation (1) and (2) reduce to (1a) and (2a):-

$$I^2 R_w - \alpha_w \sigma S_w T_w^4 - 2b_{eff} (T_w - T_s) = 0 \qquad (1a)$$

$$I^2 R_s - \alpha_s \sigma S_s T_s^4 + b_{eff} (T_w - T_s) - \frac{Ka}{L} (T_s - T_o) = 0 \qquad (2a)$$

Now when I = 1 amp, the equilibrium value of R_w is measured to be 0.45Ω. This implies a value for T_w of 930K. Substituting these values into equation (1a) gives: $2 b_{eff} (T_w - T_s) \simeq 0.41$. Using this in equation (2a) gives $T_s \sim 590K$ and hence b_{eff} is $\sim 5.9 \times 10^{-4}$ J K^{-1}.

With this value equations (1),(2) and (3) can be used to calculate the cutting wire temperature as a function of time.

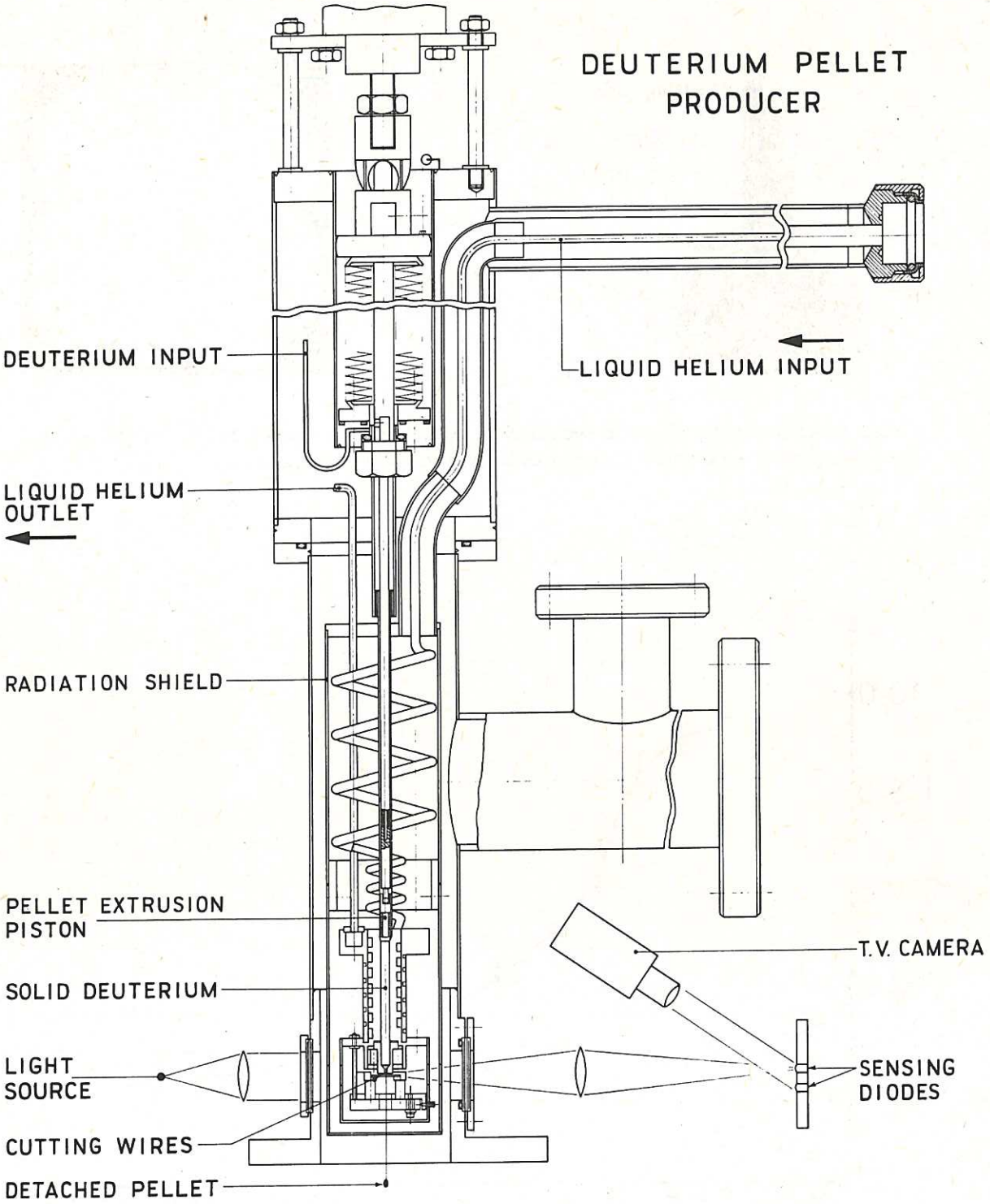

Fig.1 General diagram of the Leybold-Heraeus deuterium pellet dropper.

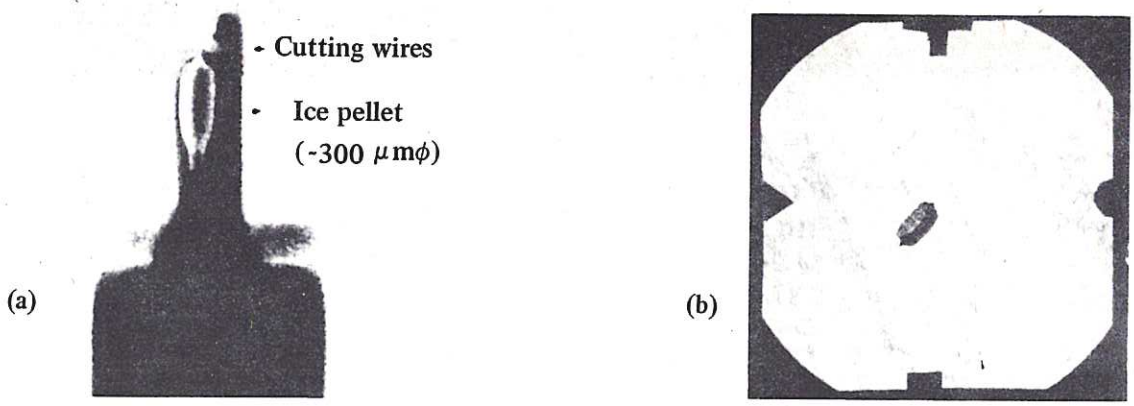

Fig.2 (a) View of pellet, shortly before detaching, as projected onto the screen. (b) Ruby laser shadowgraph (50 ns exposure) of a pellet falling through the detection point.

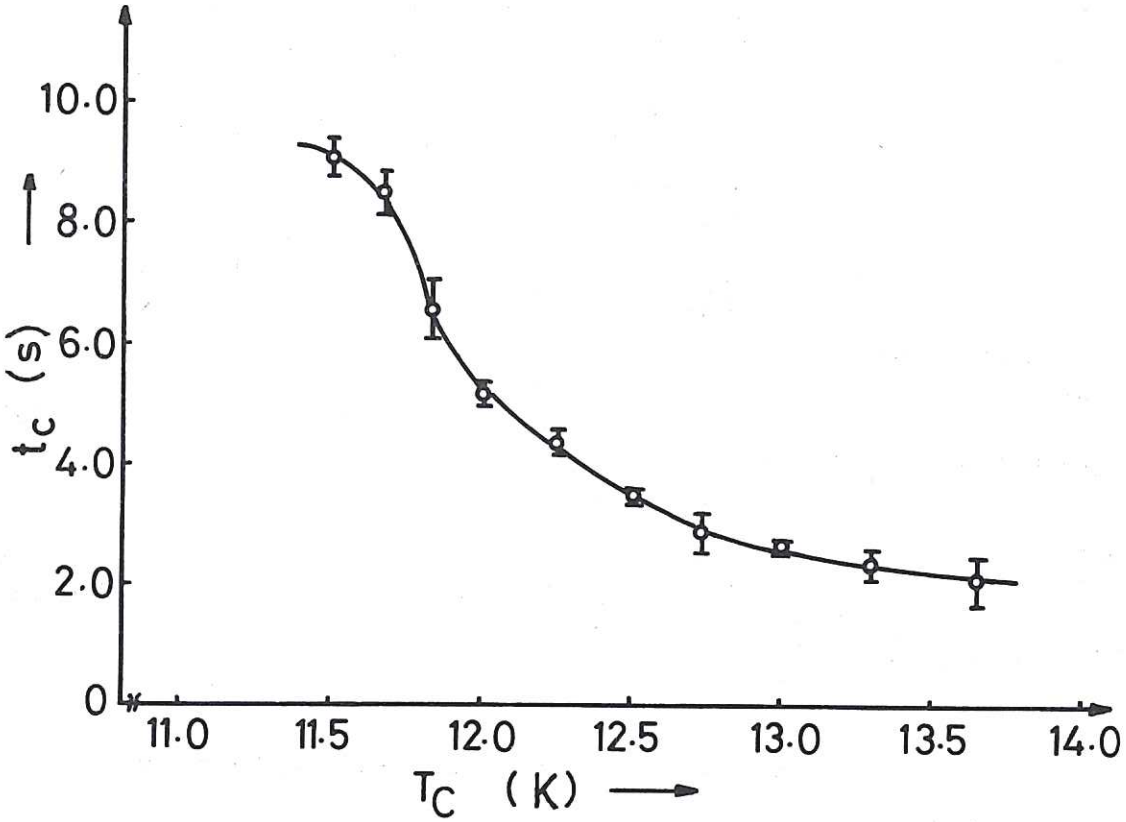

Fig.3 Variation of the delay in pellet detachment, tc, as a function of the final temperature rise, T_c. (Other temperatures and the power to the cutting wires kept constant.)

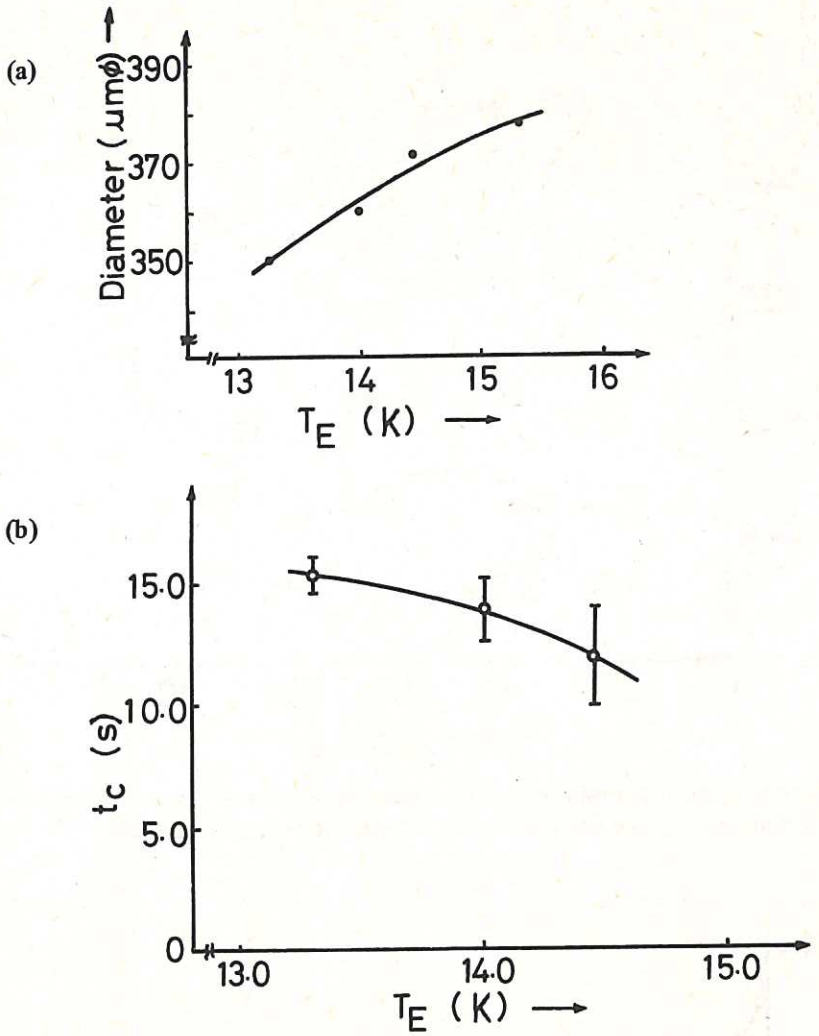

Fig.4 (a) Variation of pellet diameter with changing extrusion temperature, T_E. (b) Variation of pellet detachment delay, t_c, with changing extrusion temperature, T_E; resulting from the pellet mass dependence upon T_E implied by (a).

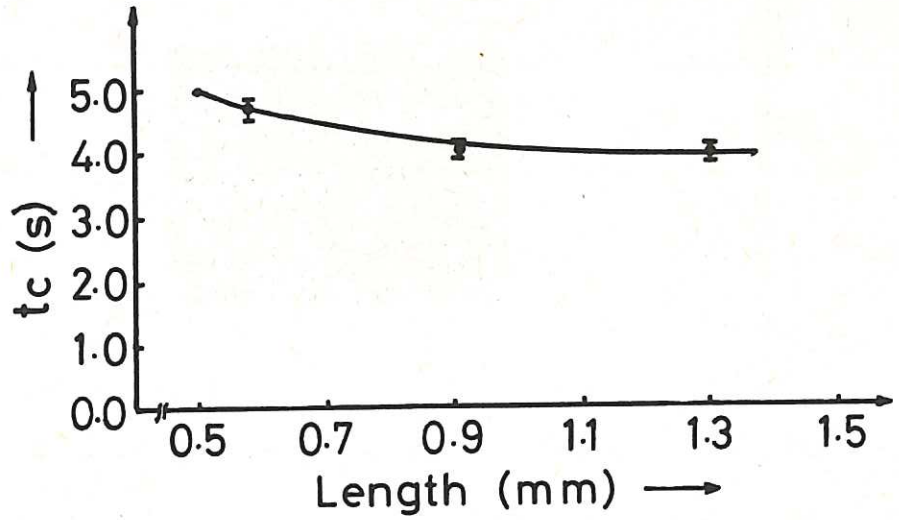

Fig.5 Variation of pellet detachment delay, t_c, as a function of pellet length.

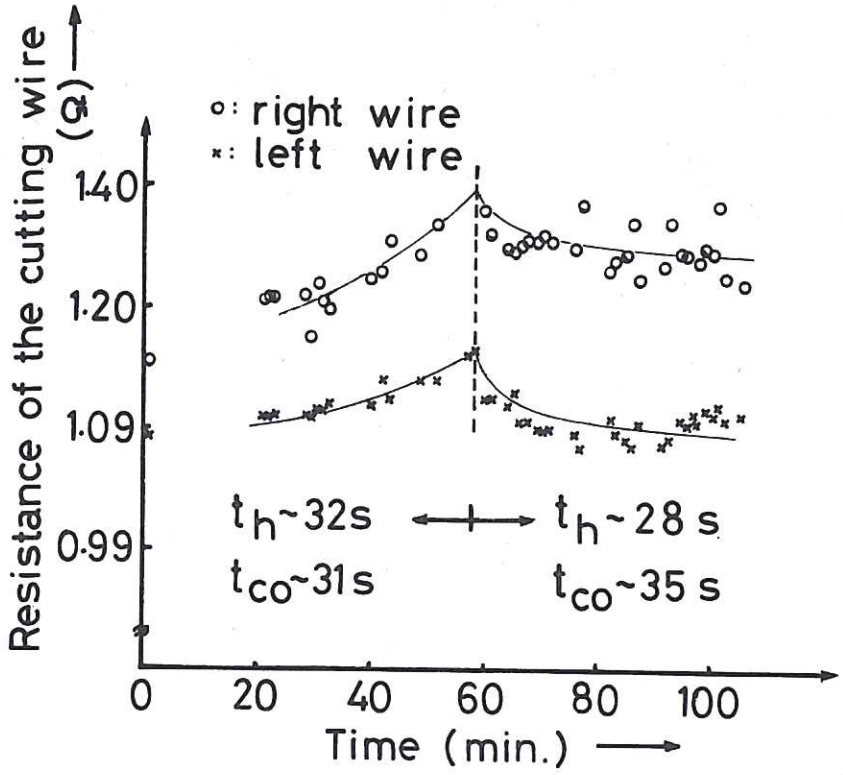

Fig.6 Variation of equilibrium value of cutting wire resistances (and hence temperature) with time. t_h refers to heating time (current on), t_{co} to cooling time (current off).

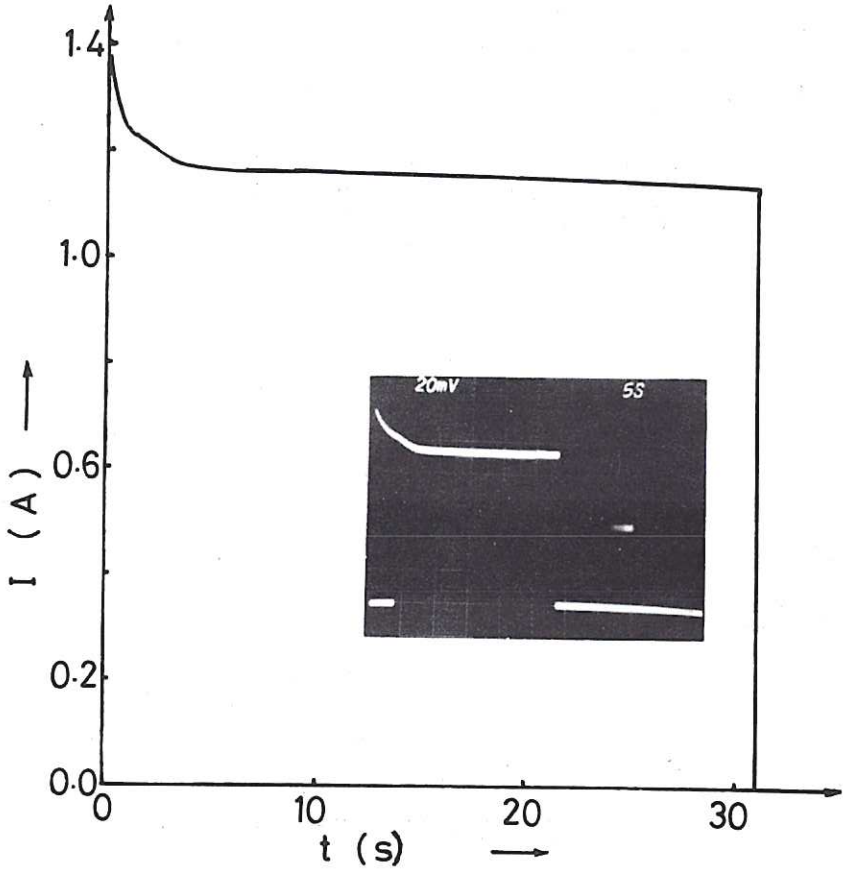

Fig.7 Theoretically calculated time profile of the cutting wire current compared to the experimentally observed time dependence (inset).

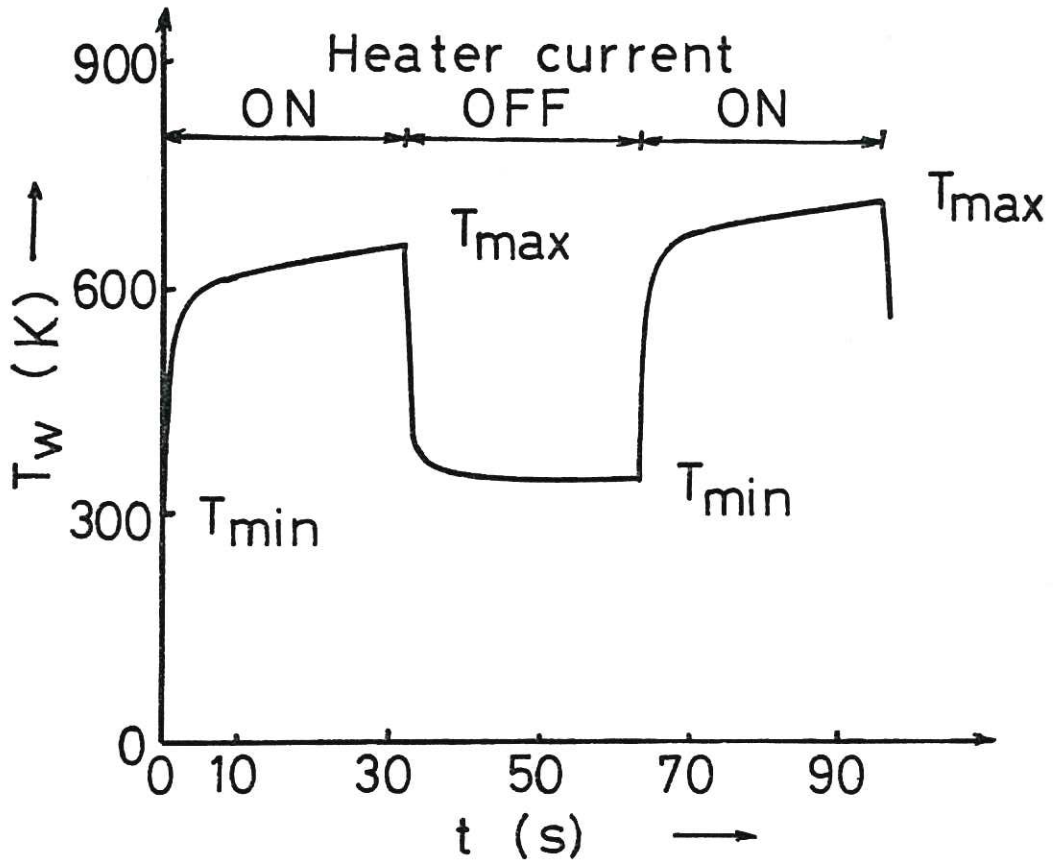

Fig.8 Theoretically calculated variation of cutting wire temperature, T_W, over two cutting cycles: showing an upward drift in temperature despite equal heating and cooling times.